International Journal of General Medicine

Dovepress
open access to scientific and medical research

Open Access Full Text Article

ORIGINAL RESEARCH

Investigation of the Mechanism of *SEMA5A* and Its Associated Autophagy-Related Genes in Gastric Cancer

Guomiao Su*, Zifan Xu*, Shiyue Liu*, Dou Hao, Yanxi Li, Guoqing Pan

Department of Pathology, the First Affiliated Hospital of Kunming Medical University, Kunming, Yunnan, People's Republic of China

*These authors contributed equally to this work

Correspondence: Guoqing Pan, Department of Pathology, the First Affiliated Hospital of Kunming Medical University, Kunming, Yunnan, People's Republic of China, Email guoqing_pan@163.com

Purpose: Semaphorin 5A (*SEMA5A*) and autophagy-related genes (ARGs) are pivotal in the pathogenesis of gastric cancer (GC). However, the potential regulatory role of *SEMA5A* in autophagy *via* its associated ARGs and the underlying molecular mechanisms remain unresolved.

Patients and Methods: GC-related datasets from The Cancer Genome Atlas (TCGA) and Gene Expression Omnibus (GEO) were analyzed to identify differentially expressed genes (DEGs) between GC and control samples. The intersection of DEGs with ARGs produced candidate genes, which were further analyzed using Spearman correlation with *SEMA5A* to identify signature genes. Stratification of GC samples based on signature gene expression, followed by Kaplan-Meier survival analysis, identified key genes. Subsequent analyses, including gene set enrichment analysis (GSEA), immune infiltration, and immune checkpoint evaluation, were conducted on the key genes and *SEMA5A*. The mRNA expression level was quantified using real-time quantitative polymerase chain reaction (RT-qPCR).

Results: Ninety candidate genes were identified for Spearman correlation with *SEMA5A*, revealing *TNFSF11, BMP6, ITPR1*, and *DLC1* with correlation coefficients exceeding 0.3. Survival analysis underscored *DLC1* and *BMP6* as key genes due to significant prognostic differences. GSEA implicated *SEMA5A, BMP6*, and *DLC1* in the ECM receptor interaction pathway. Immune infiltration analysis indicated a negative correlation of *SEMA5A* and *BMP6* with M1 macrophages, while *DLC1* exhibited the strongest association with the immune checkpoint *PDCD1LG2* ($p < 0.05$, cor = 0.43). The mRNA expression level of *SEMA5A* was significantly upregulated in AGS parental cells compared to GES-1 cells ($p < 0.01$), whereas *DLC1* and *BMP6* mRNA levels were markedly downregulated in AGS parental cells relative to GES-1 ($p < 0.0001$).

Conclusion: ARGs *BMP6 and DLC1*, associated with *SEMA5A*, were identified, and their prognostic significance in GC was demonstrated. Additionally, their regulatory mechanisms were further elucidated through immune infiltration analysis and molecular network construction, providing a theoretical foundation for future research on the molecular mechanisms in patients with GC.

Keywords: GC, SEMA5A, autophagy, ARGs, bioinformatics analysis

Introduction

Gastric cancer (GC) ranks as one of the most common malignancies globally, holding the fifth position in both morbidity and mortality.[1] In China alone, approximately 480,000 incidence cases of GC and 370,000 related deaths occur annually, representing nearly half of the global burden of this disease. Despite notable advancements in GC research and clinical treatment, the majority of patients are diagnosed at an advanced stage, resulting in a 5-year survival rate of less than 20%.[2] Therefore, it is imperative to explore the risk factors and carcinogenic mechanisms associated with GC and to strengthen preventive measures and treatment strategies to lower the incidence and mortality rates.

Semaphorin 5A (*SEMA5A*), located on human chromosome 5p15.2, is a member of the semaphorin family, initially recognized for its role in central nervous system development across various species. *SEMA5A* exerts a repulsive effect

Received: 4 June 2024
Accepted: 27 August 2024
Published: 14 September 2024

on neuronal axons, guiding their growth and preventing misrouting. While primarily identified as a nerve axon guidance molecule, its role in human tumorigenesis has been less studied.[3] Our research group found that *SEMA5A* is upregulated in GC tissues and cells, where it promotes invasion and metastasis through the ERK/MMP9 and PI3K/Akt/uPA signaling pathways.[4–7]

Autophagy, a highly conserved process present in nearly all eukaryotic cells, plays a critical role in various physiological and pathological conditions, including maintaining cellular homeostasis, DNA damage repair, and regulating metastasis in malignant tumors.[8,9] Depending on the mechanism of lysosomal substrate transport, autophagy is categorized into macroautophagy, microautophagy, and molecular chaperone-mediated autophagy, with macroautophagy being the most extensively studied.[10]

Autophagy, a critical mechanism for maintaining cellular homeostasis, significantly influences the pathogenesis and progression of various malignant tumors, including GC.[11] Research has shown that stomach cancer cells exhibit markedly elevated levels of autophagy, where essential substances necessary for GC cell survival are degraded, hindering the uptake of nutrients vital for their growth and division, ultimately leading to tumor cell death. This process represents an intrinsic inhibitory mechanism against tumor progression. The suppressive effect of autophagy on GC is further demonstrated by its ability to induce autophagy and mediate apoptosis, thereby effectively inhibiting GC cell proliferation. Conversely, the inhibition of autophagy may facilitate the onset and metastasis of GC.[12,13] Currently, the potential role of *SEMA5A* in mediating autophagy in GC, and the nature of its involvement, remains unreported in the literature, requiring further investigation and validation. Bioinformatics technology is increasingly utilized in the prognostic and mechanistic analysis of cancer. Gao et al[14–16] through bioinformatics analysis, identified key pathways affecting the survival and prognosis of patients with cancers, unveiling new biomarkers and therapeutic targets for cancer diagnosis, treatment, and prognostic evaluation, thus laying the foundation for more effective anti-gastrointestinal tumor strategies.

This study aims to investigate the regulatory mechanisms and immune microenvironment associated with *SEMA5A* and its related ARGs in GC through bioinformatics analysis, offering novel insights for the diagnosis, treatment, and prognosis of patients with GC.

Materials and Methods

Data Extraction

The Gene Expression Omnibus (GEO) database (https://www.ncbi.nlm.nih.gov/geo/) and The Cancer Genome Atlas (TCGA) database (https://tcga-data.nci.nih.gov/tcga/) were the sources of the GC-related datasets. The TCGA database was used to obtain the transcriptome data associated to GC (including count and FPKM data), clinical, and survival information. After removing duplicate patient samples, the TCGA-GC contained 373 GC samples and 32 normal samples. To find DEGs, the TCGA-GC dataset was used. The external validation set GSE118916, comprising of 15 normal samples and 15 GC samples, was used to verify the DEGs. A total of 757 ARGs were collected after duplicate genes were removed from the Gene Set Enrichment Analysis (GSEA) website (https://www.gsea-msigdb.org/gsea/index.jsp) and the Human Autophagy Database (HADb, http://www.autophagy.lu/index.html).

Correspondence Analysis of the SEMA5A Gene

We divided the GC samples into two categories: high expressed gene groups and low expressed gene groups based on the ideal threshold of expression, which were determined by the *SEMA5A* gene's expression levels in the training set. We next assessed the predictive importance of *SEMA5A* in these two groups using Kaplan-Meier (K-M) survival analysis. Furthermore, we assessed the expression of the *SEMA5A* gene among GC samples with varying clinicopathological characteristics, taking into account the gender, age, TNM staging, and cancer stage of the GC patients in the training set. With the "DESeq2 (Version1.38.3)" and "Limma" packages, we assessed the expression of the *SEMA5A* gene in the GC group compared to the normal group in the TCGA-GC and GSE118916, respectively.[17]

Identification of Candidate Genes

In this research, the differential expression genes (DEGs) in the training set between the GC and control groups were compared using the R programming language's "DESeq2 (Version 1.38.3)".[18] The criteria for screening were p adj < 0.05 and |log2FC| > 1. Additionally, candidate genes were produced by joining ARGs and DEGs.

Functional Enrichment Analysis of Candidate Genes

To understand the main metabolic and signaling pathways that are influenced by candidate genes. Using the "clusterProfiler (Version 4.4.4)" package, candidate genes were subjected to enrichment analyses for Kyoto Encyclopedia of Genes and Genomes (KEGG) and Gene ontology (GO) in order to find shared functions and linked pathways.[19] Molecular functions (MF), biological processes (BP), and cellular components (CC) make up the three parts of the GO system. For both KEGG and GO enrichment analyses, the screening criterion of $p<0.05$ was applied, and the same cutoff was employed.

Identification of Key Genes

Using the *SEMA5A* gene as a candidate, we performed a spearman analysis. The study's signature genes were found using the standards of $|cor|>0.3$ and $p<0.05$. Using the ideal threshold of the signature gene expression levels, we separated the GC samples in the training set into groups with high expressed genes and low expressed genes. We used the "survival (Version 3.4–0)" program to perform K-M survival analysis on these groups in order to assess the predictive importance of each signature gene. Next, key genes were identified from the genes that showed substantial changes in survival between the high and low expression groups. Following that, the training set's key genes' expression trends and associations with *SEMA5A* were examined. Finally, based on a number of clinicopathological characteristics, including gender, age, cancer stage and TNM staging, the expression difference of key genes in different clinicopathological features was further explored.

Gene Set Enrichment Analysis (GSEA)

GO and KEGG enrichment analysis was performed using the R package "org.Hs.eg.db (Version 3.15.0)" and the R package "clusterProfiler" (Version 4.4.4) to investigate the biological mechanisms and signaling pathways linked to the *SEMA5A* gene and key genes.[20] The reference datasets for the GSEA analysis were the GO: c5.go.v2022.1.Hs.entrez.gmt and KEGG: c2.cp.kegg.v2022.1.Hs.entrez.gmt gene set files, which were downloaded from the official GSEA website. Based on the median value of *SEMA5A* expression, GC samples were divided into groups for high expressed genes and low expressed genes. Following this, GSEA enrichment analysis was performed on all the genes in the categories of high expressed genes and low expressed genes, sorting the results based on differential gene expression. The following criteria were used to rank the analysis results: $|NES| > 1$, NOM $p < 0.05$, and $q < 0.25$.

Analysis of the Immune Microenvironment

Disease development is significantly influenced by alterations in the immunological environment of the body. To monitor the immune cell composition in the samples, we used CIBERSORT to assess the samples for immune infiltration. The differences in immune cell infiltration between the disease and normal groups, as well as between the groups with high and low expression of *SEMA5A, BMP6*, and *DLC1*, were compared using a *t*-test. The relationship between *SEMA5A* and key genes with distinct immune cells in each group was investigated using the spearman method. The differences in the expression of the eight immunological checkpoints between the groups of *SEMA5A* genes with high and low expression were next assessed, as well as the correlation of *SEMA5A* and key genes with differential immune checkpoints. Furthermore, in groups of high- and low-expressed genes, the ESTIMATEScore, ImmuneScore, and StromalScore were calculated using the ESTIMATE algorithm.

Construction of miRNA-mRNA-TF Network of Signature Genes

Through the use of microRNA response elements, co-construction of competitive endogenous RNA (ceRNA) networks can provide insight into interactions between various RNA molecules. To gain further insight into the function of important

genes in the onset and progression of disease. Competitive endogenous RNAs (ceRNAs) were created in this work to investigate the molecular processes of important genes. First, using the PicTar (http://pictar.mdc-berlin.de) and miRmap (https://mirmap.ezlab.org) databases, miRNAs for important genes were predicted. Next, based on clipExpNum ≧20, the lncRNA related to miRNA was predicted. Next, the mirnet database (https://www.mirnet.ca) was used to determine the transcription factors of important genes. Lastly, the TF-mRNA network of important genes and the ceRNAs regulatory network were built, respectively.

Cell Culture

In RPMI 1640 media, GES-1 and AGS were cultivated at 37°C, 5% CO2, and 10% PBS. Suzhou Hysigen Biotechnology Co., Ltd. was sold GES1. Wuhan Procell Life Sciences Co. was sold to AGS.

Real-Time Quantitative polymerase Chain Reaction (RT-qPCR)

Total RNA was extracted from cell line using Trizol reagent (Invitrogen). In accordance with the instructions, 5 μg of total RNA were used to create 10 μL of cDNA. The first cycle of RT-qPCR is conducted at 95°C with a 15-minute pre-denaturation period. Cycle 2: reaction, 95°C for 30 seconds, 60°C for 60 cycles. Cycle 3: Dissociation at 95°C; Cycle 4: Dissolution curve at 95°C. The RT-qPCR primers utilized were listed in Table 1. The relative expression of the RNA of interest was calculated using the $2^{-\Delta\Delta Ct}$ method.

Statistical Analysis

R software was used for all bioinformatics analysis in this study. An ANOVA was used to evaluate the RT-qPCR results. A difference that was deemed significant was one with $p<0.05$.

Results

SEMA5A Was Correlated with GC Prognosis

To assess the role of the *SEMA5A* gene in GC, its expression levels were compared between the GC and control groups. Figure 1A and B reveals significant differences in *SEMA5A* expression, with elevated levels observed in the GC group of the training set, while the control group exhibited lower levels. This expression pattern in the validation set was consistent with that of the training set. Kaplan-Meier survival analysis indicated that patients with higher *SEMA5A* expression had a significantly poorer prognosis, in contrast to those with lower expression (Figure 1C).

Table 1 Primer Sequences for RT-qPCR

Genes	Primer Sequences
SEMA5A	F:5'-AAGATCCAGTAGCGTAGAAGAG-3'
	R:5'-TGTTGATGTGGTTGGTTATGC-3'
DLC1	F:5'-GATCACTGAAGCAACGCAACC-3'
	R:5'-ACAGACCCTCAACAAACAGGA-3'
BMP6	F:5'-GTCAGCGACACCACAAAGAG-3'
	R:5'-ACACAGTCCTTGTAGATGCGG-3'
GAPDH	F:5'-TGTTGCCATCAATGACCCCTT-3'
	R:5'-CTCCACGACGTACTCAGCG-3'

Abbreviations: ARGs, autophagy-related genes; GC, gastric cancer; TCGA, Cancer Genome Atlas; GEO, gene expression omnibus; DEGs, differential expression genes; GSEA, gene set enrichment analysis; RT-qPCR, real-time quantitative polymerase chain reaction; HAD, human Autophagy; GSEA, gene set enrichment analysis; KEGG, Kyoto Encyclopedia of Genes and Genomes; CC, cellular components; MF, molecular functions; BP; biological process; ceRNA, competitive endogenous RNAs.

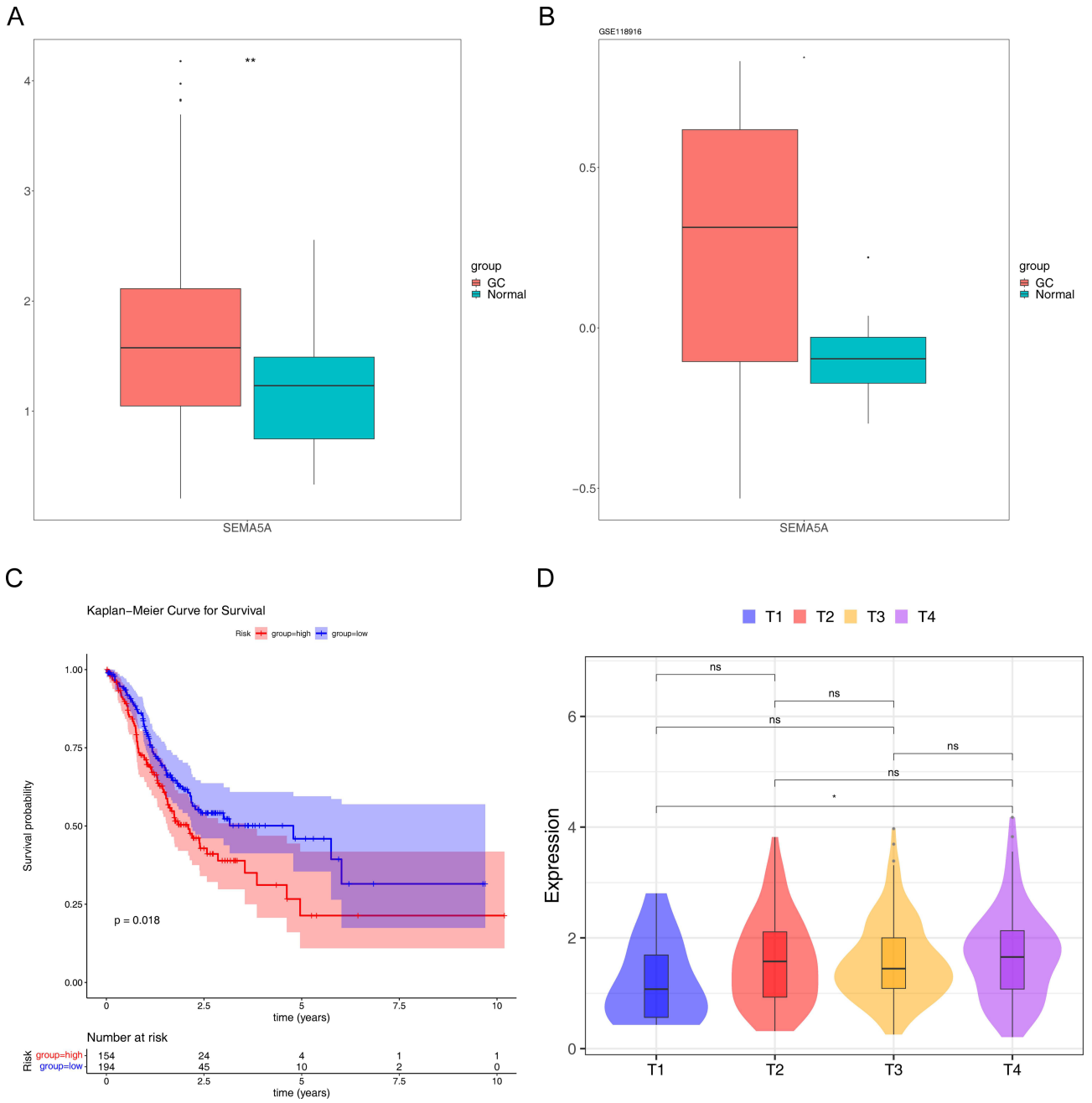

Figure 1 The prognostic performance of the EMA5A gene is identified. (**A**)The TCGA dataset's EMA5A gene expression levels. (**B**)The EMA5A gene's expression levels in GSE118916 . (**C**) Kaplan-Meier survival curves for the *SEMA5A* gene in the TCGA dataset for high and low expression groups. (**D**)The EMA5A gene's expression levels in clinicopathological traits (T stages). ns, no significance; * $p < 0.05$; ** $p < 0.01$; *** $p < 0.001$. **** $p < 0.0001$.

Additionally, the relationship between *SEMA5A* expression and various clinicopathological features in the training set was examined, including gender, age, cancer stage, and TNM staging. The analysis, illustrated in Figure 1D, highlighted a notable difference in *SEMA5A* expression between T1 and T4 stages.

Identification of Candidate Genes

Following a differential analysis between GC and control samples, 5235 DEGs were identified, with 2683 genes upregulated and 2552 downregulated (Figure 2A and B). These DEGs were then intersected with ARGs, yielding 90 candidate genes (Figure 2C).

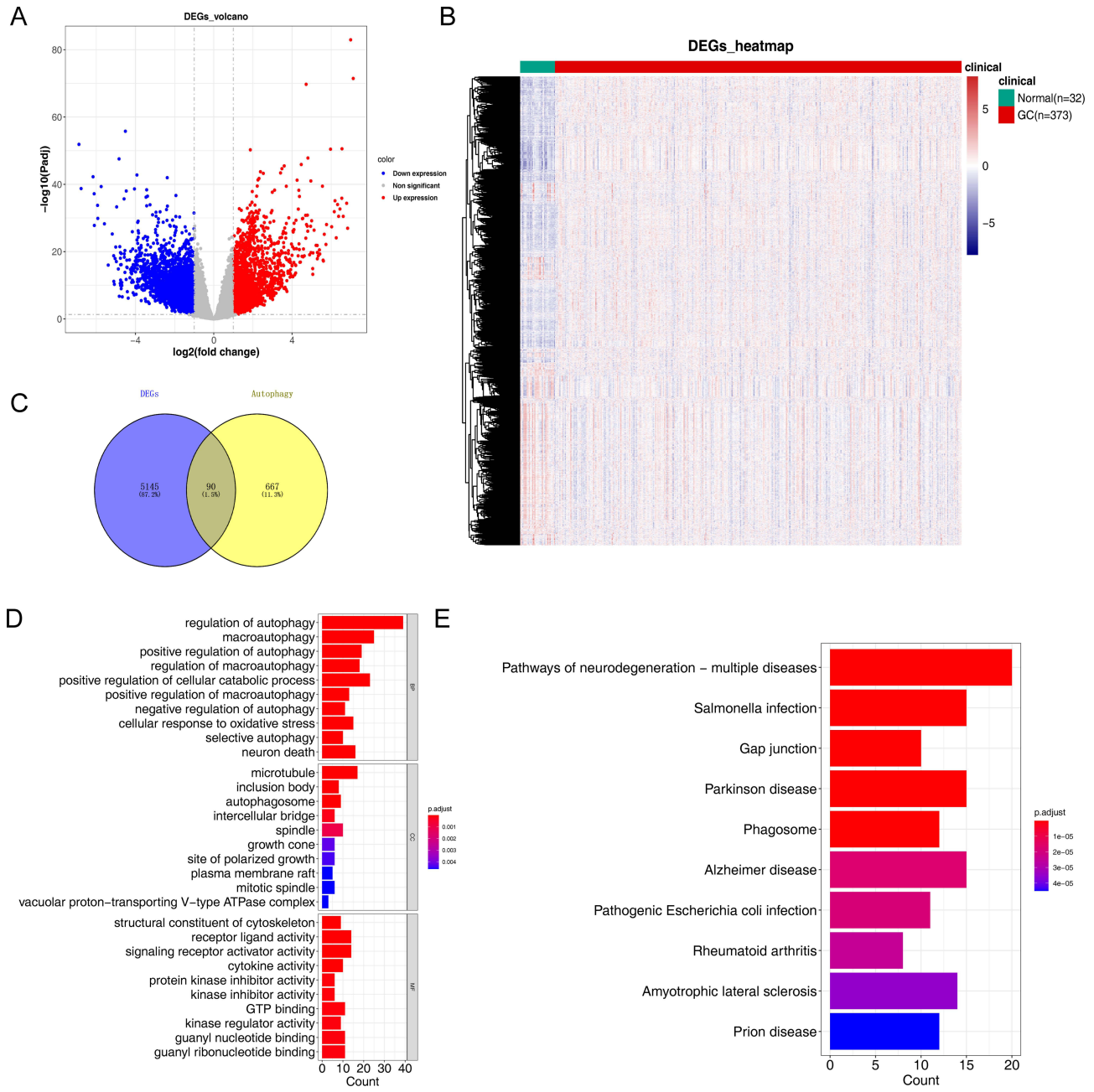

Figure 2 Candidate genes linked to autophagy in GC identified. (**A**) The Volcano plot from differential expression analysis; blue indicates down-regulated gene expression and red indicates up-regulated gene expression. (**B**) A heatmap showing the genes that differ in expression (DEGs) between the GC and control groups in the TCGA dataset. (**C**) A Venn diagram used to identify potential genes. (**D**) GO and (**E**) Candidate of potential genes' KEGG enrichment.

Functional investigation of these candidate genes was conducted through GO and KEGG analyses. The GO enrichment analysis results, presented in Figure 2D, revealed that, in terms of biological processes, the candidate genes were associated with autophagy regulation, positive regulation of cellular catabolic processes, macroautophagy, and cellular responses to oxidative and chemical stress. Regarding cellular components, significant enrichment was observed in microtubules, intercellular bridges, polarized growth sites, plasma membrane rafts, and vacuolar proton-transporting V-type ATPase complexes. For molecular functions, the candidate genes were notably enriched in categories such as structural constituents of the cytoskeleton, receptor-ligand activity, signaling receptor activator activity, cytokine activity, and protein kinase inhibitor activity. KEGG analysis indicated significant enrichment of the candidate genes in pathways related to neurodegeneration, including various diseases, Salmonella infection, Pathogenic Escherichia coli

infection, Amyotrophic lateral sclerosis, Cytokine-cytokine receptor interaction, EGFR tyrosine kinase inhibitor resistance, and Prion disease (Figure 2E).

BMP6 and DLC1 Were Identified as Key Genes

To identify signature genes, the candidate genes were analyzed using Spearman correlation with *SEMA5A*. Four genes (*TNFSF11, BMP6, ITPR1*, and *DLC1*) satisfied the criteria of |cor|>0.3 and $p < 0.05$ and were designated as signature genes for further analysis. As illustrated in Figure 3A, all signature genes exhibited a significant positive correlation with *SEMA5A*.

GC samples in the training set were categorized into high and low expression groups based on the optimal threshold of signature gene expression levels. Kaplan-Meier survival analysis revealed significant prognostic differences between the high and low expression groups for *DLC1* and *BMP6*. However, no significant differences were observed between the expression groups for *TNFSF11* and *ITPR1* (Figure 3B–E). Consequently, *BMP6* and *DLC1* were identified as key genes. Notably, both *DLC1* and *BMP6* were significantly downregulated in the GC groups and showed a strong correlation with *SEMA5A* (*BMP6*: $p < 0.05$, cor = 0.3315; *DLC1*: $p < 0.05$, cor = 0.3816) (Figure 3F and G). Additionally, significant differences in *BMP6* and *DLC1* expression were observed across T-stage groups (Figure 3H).

SEMA5A, BMP6, and DLC1 Were Both Enriched in the ECM Receptor Interaction Pathway

To explore the potential biological functions of *SEMA5A* and key associated genes, GSEA was performed. The *SEMA5A* gene was enriched in 1676 GO terms and 52 KEGG pathways. From these, the top 5 most significant GO terms (eg, B cell receptor signaling pathway, collagen fibril organization) and KEGG pathways (eg, ECM-receptor interaction, focal adhesion) were selected for visualization (Figure 4A and B). For the *BMP6* gene, enrichment analysis revealed its involvement in 2456 GO terms and 79 KEGG pathways. The top 5 significant GO terms (eg, phagocytosis recognition, immunoglobulin complex) and KEGG pathways (eg, cell adhesion molecules CAMs, ECM-receptor interaction) were mapped (Figure 4C and D). Similarly, enrichment analysis of the *DLC1* gene identified its presence in 2126 GO terms and 69 KEGG pathways. The top 5 significant GO terms (eg, muscle contraction, collagen-containing extracellular matrix) and KEGG pathways (eg, ECM-receptor interaction, focal adhesion) were selected for mapping (Figure 4E and F).

The Correlation of Key Genes with Immune Cells and Immune Checkpoints

To investigate the immune microenvironment in patients with GC, an immune infiltration analysis was conducted. Using the CIBERSORT algorithm, the infiltration abundance of 22 immune cell types in GC and control samples was calculated in the training set (Figure 5A). Among these, 12 cell types exhibited significant differences between the GC and control groups (Figure 5B). Additionally, significant differences were observed in 4, 7, and 4 immune cell types between the high and low expression groups of *SEMA5A, BMP6*, and *DLC1*, respectively (Figure 5C–E). Further analysis of the correlation between key genes, including *SEMA5A*, and the differentially infiltrated cells across various groups revealed that *SEMA5A* and *BMP6* were negatively correlated with M1 macrophages (Figure 5F–I).

In this study, the expression levels of 8 immune checkpoints were also compared between the high and low expression groups of *SEMA5A*. The high expression group exhibited significantly higher levels of HAVCR2 and PDCD1LG2 compared to the low expression group (Figure 6A). Furthermore, *DLC1, BMP6*, and *SEMA5A* were significantly associated with two different immune checkpoints, with *DLC1* showing the strongest positive correlation with PDCD1LG2 ($p < 0.05$, cor = 0.43) (Figure 6B). Additionally, the ESTIMATE, Immune, and Stromal Scores were significantly elevated in the high expression group (Figure 6C).

The ceRNA and TF-mRNA Network for SEMA5A, BMP6, and DLC1 Were Constructed

To systematically identify the ceRNAs and TF-mRNA interactions involved in the gene expression regulation of *SEMA5A, BMP6*, and *DLC1*, and to elucidate the relationships among these components, a computational approach was employed. Using

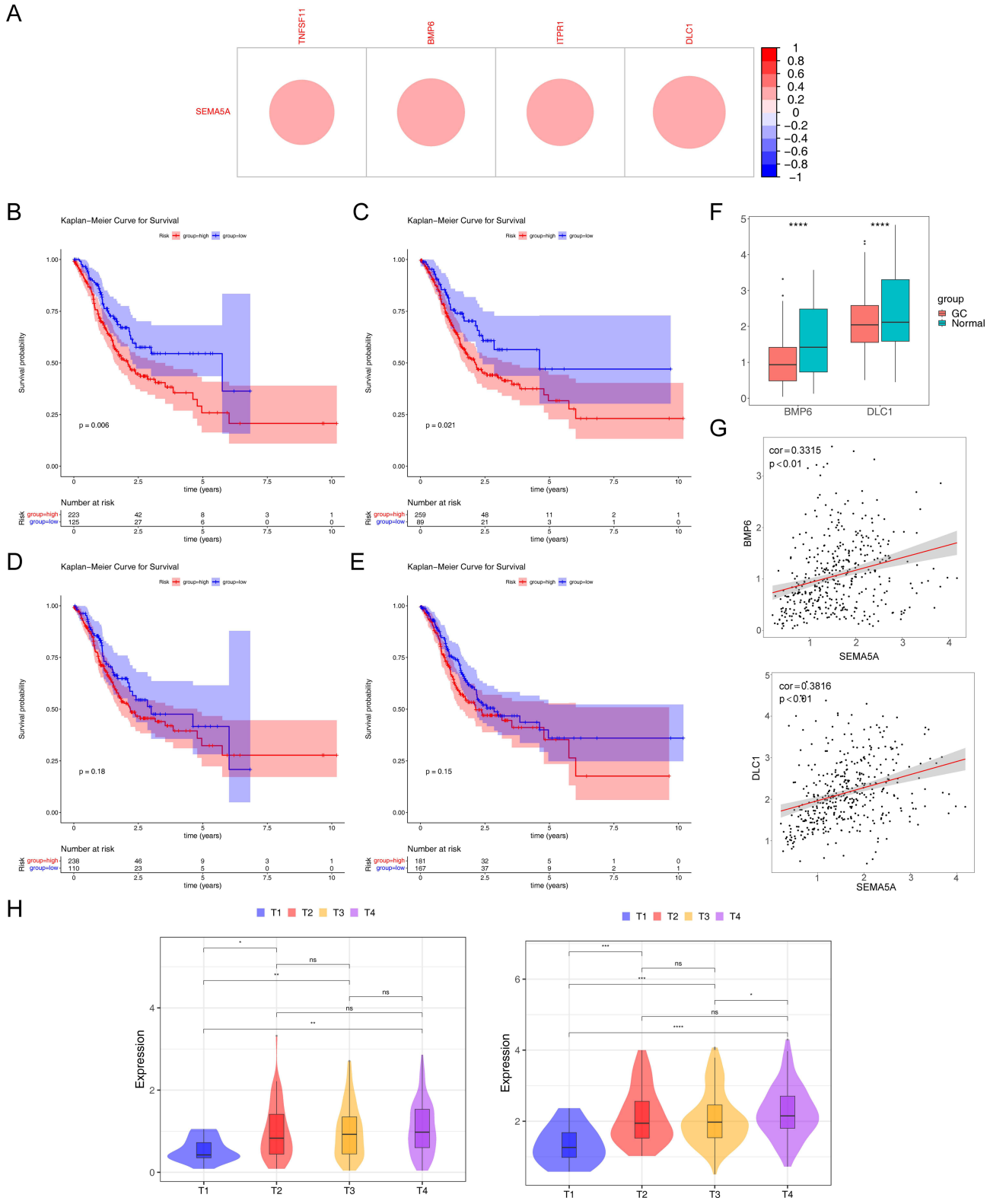

Figure 3 Acquisition of important genes and study of their connection with clinicopathological features. (**A**) The SEMA5A gene and candidate gene were correlated; the wider the circle, the stronger the association. Red indicated positive correlation and blue represented negative correlation. The Kaplan-Meier survival curves of the signature genes (**B**) DLC1, (**C**) BMP6, (**D**) ITPR1, and (**E**) TNFSF11 in the TCGA dataset, showing high (red) and low (blue) expression groups, respectively. (**F**) The TCGA dataset's DLC1 and BMP6 expression levels. (**G**) An examination of the association between DLC1, BMP6, and SEMA5A. (**H**): The BMP6 and DLC1 gene expression levels in clinicopathological features (T stages). * $p < 0.05$; ** $p < 0.01$; *** $p < 0.001$.**** $p < 0.0001$.

Abbreviation: ns, no significance.

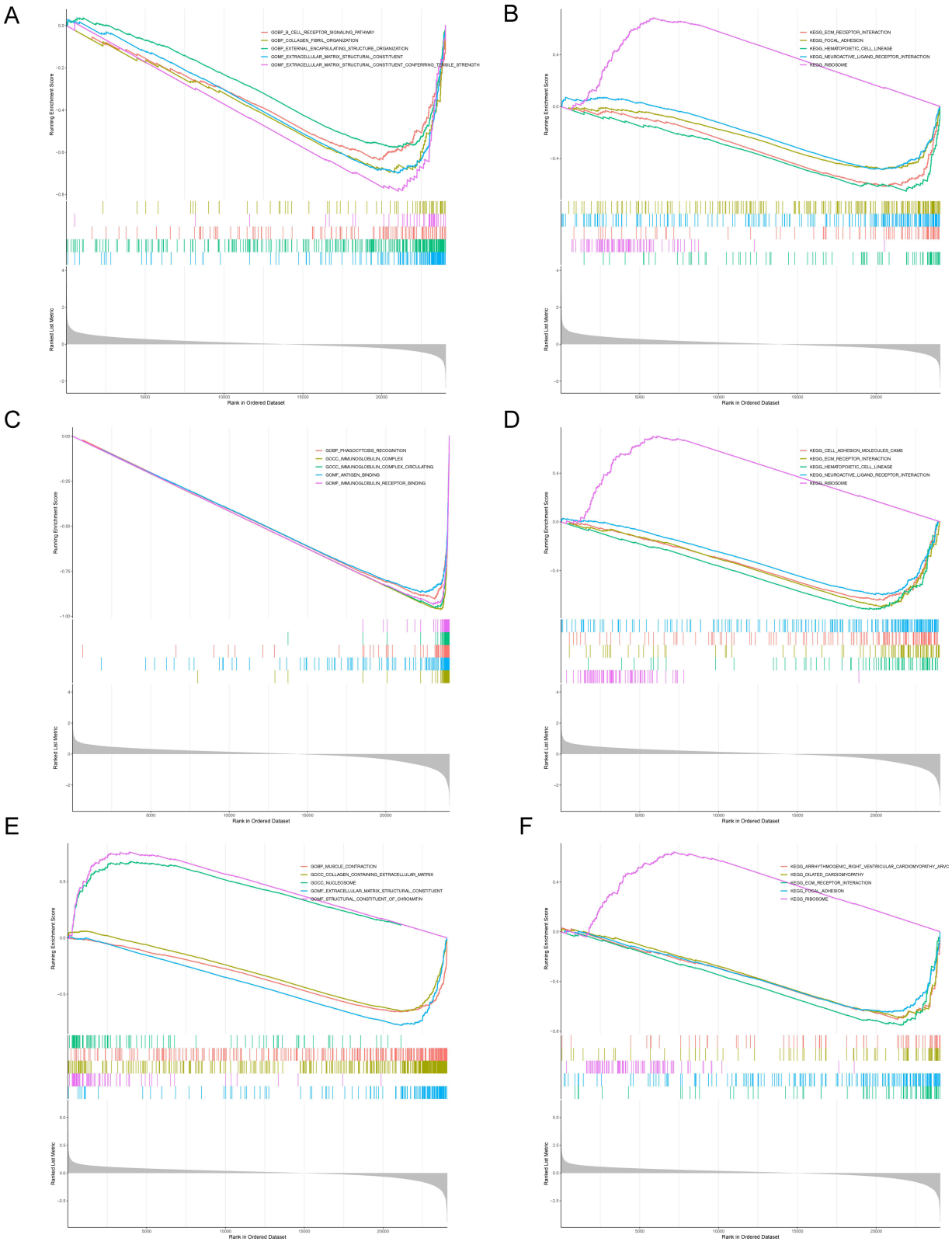

Figure 4 *SEMA5A*, *BMP6*, and *DLC1* gene sets enrichment analysis (GSEA). (**A**) GO and (**B**) KEGG enrichment analyses of SEMA5A, respectively. BMP6's (**C**) GO and (**D**) KEGG enrichment analyses, respectively. (**E**) GO and (**F**) KEGG enrichment analysis of DLC1, respectively. * $p < 0.0001$; ** $p < 0.01$; *** $p < 0.001$.
Abbreviation: ns, no significance.

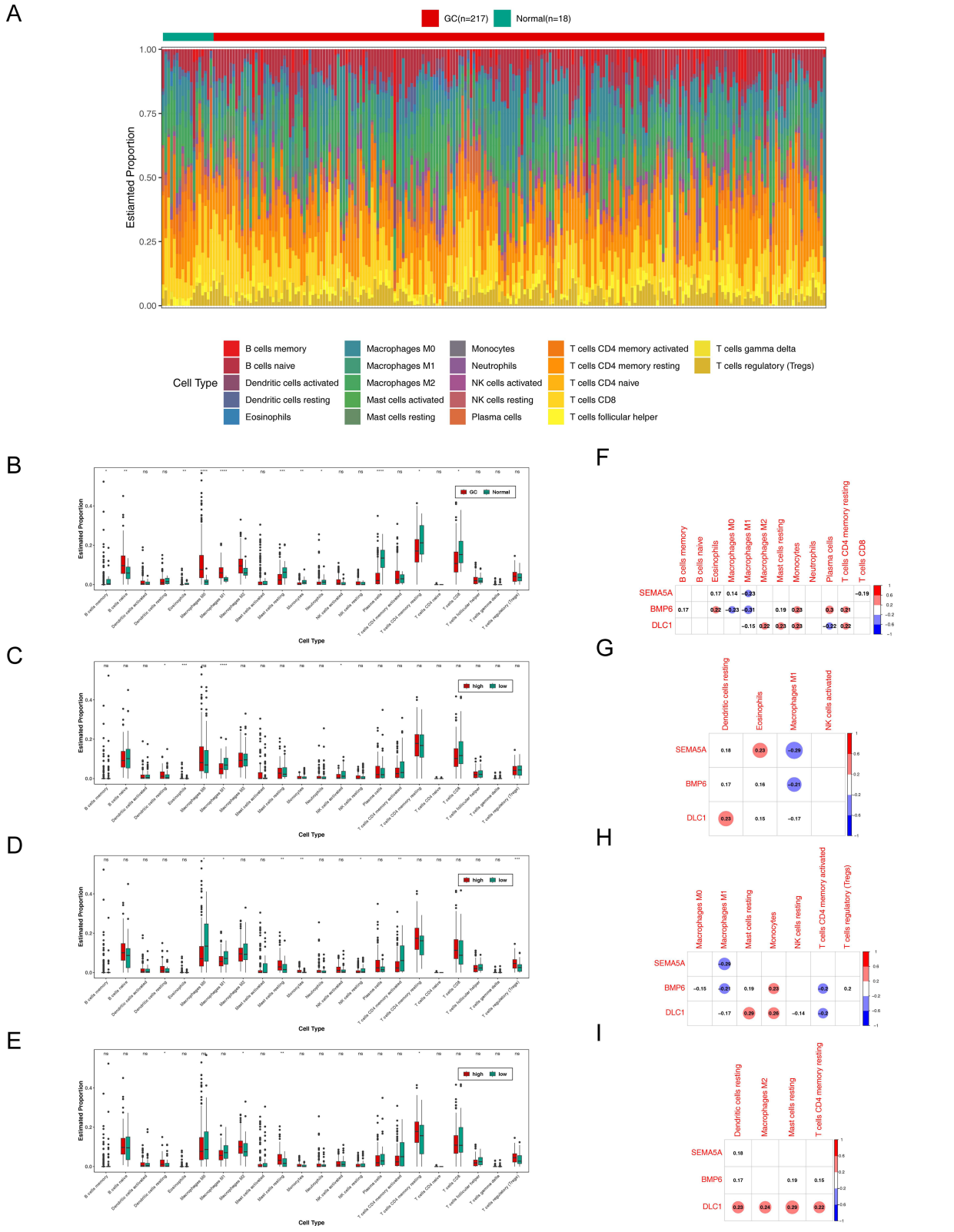

Figure 5 Comparison of immune cell infiltration between several groups (**A**) The heat map displayed the number of immune cells that infiltrated the GC (red) and control (green) samples in the TCGA dataset. (**B**) The GC (red) and control (green) groups differed significantly in 12 immune cells. (**C**) Variations in immune cells between *SEMA5A* gene high and low expression groups; (**D**) *BMP6* gene; and (**E**) *DLC1* gene. (**F**) A comparison of the GC and control groups' *SEMA5A, BMP6, DLC1*, and differential immune cells. The investigation of the link between *SEMA5A* and differential immune cells in the high and low expression groups of the genes *BMP6, DLC1*, and *SEMA5A* (**G**), (**H**), and (**I**). The wider the circle, the stronger the association; red denoted positive correlation while blue indicated negative correlation. * $p < 0.05$; ** $p < 0.01$; *** $p < 0.001$.**** $p < 0.0001$.
Abbreviation: ns, no significance.

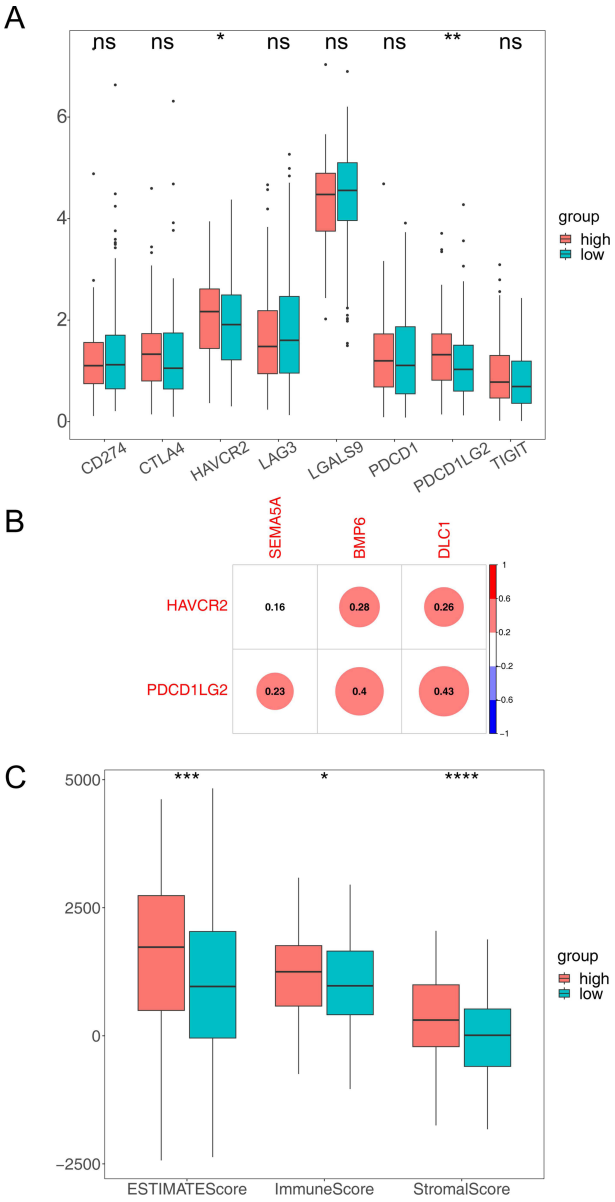

Figure 6 ESTIMATE analysis and immune checkpoint analysis. (**A**): The GC and control groups differed significantly at both immunological checkpoints. (**B**): The differential checkpoint's association study with *SEMA5A, BMP6*, and *DLC1*. The wider the circle, the stronger the association; red denoted positive correlation while blue indicated negative correlation. (**C**): ESTIMATE scores in the high and low expression groups plotted on a box line. * $p < 0.05$; ** $p < 0.01$; *** $p < 0.001$.**** $p < 0.0001$.
Abbreviation: ns, no significance.

the PicTar and miRmap databases, 34 miRNAs potentially associated with *SEMA5A, BMP6*, and *DLC1* were predicted. Additionally, 44 lncRNAs were identified to interact with these miRNAs based on a clipExpNum threshold of ≥ 20. Subsequently, a ceRNA regulatory network was constructed, including interaction pairs such as NEAT1-hsa-miR-5195-3p-*DLC1* and SNHG16-hsa-let-7d-5p-*SEMA5A* (Figure 7A). Finally, 29 transcription factors (TFs) were predicted to correspond to *SEMA5A, BMP6*, and *DLC1*, forming 37 interactions within the TF-mRNA network, including pairs such as RELA-*DLC1* and FOXL1-*BMP6* (Figure 7B).

Verification of Gene Expression from Cells

In vitro studies analyzed the mRNA levels of the three genes in human gastric adenocarcinoma cells (AGS) compared to normal human gastric mucosal cells (GES-1). The results demonstrated that *SEMA5A* mRNA expression was significantly upregulated in AGS parental cells compared to GES-1 cells (Figure 8A). Conversely, the mRNA expression levels of *DLC1* and *BMP6* were downregulated in AGS parental cells relative to GES-1 cells (Figure 8B and C).

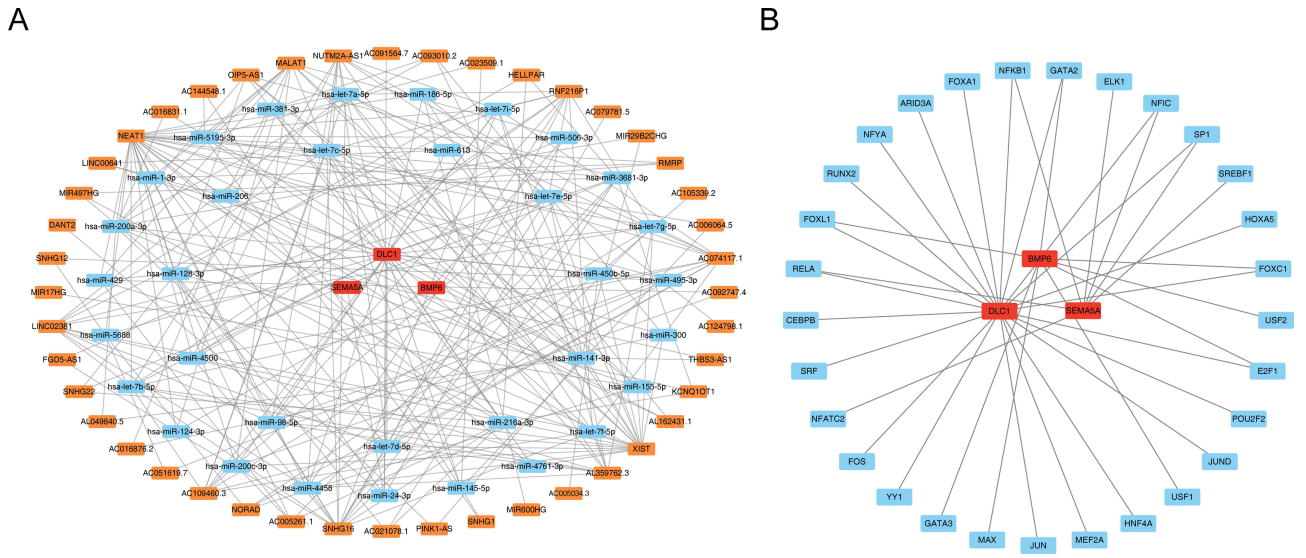

Figure 7 *SEMA5A*, *BMP6*, and *DLC1* regulatory networks being constructed. (**A**) The SEMA5A, BMP6, and DLC1 ceRNA networks. (**B**) The *SEMA5A*, *BMP6*, and *DLC1* TF-mRNA networks. A reciprocal relationship is indicated by connected lines.

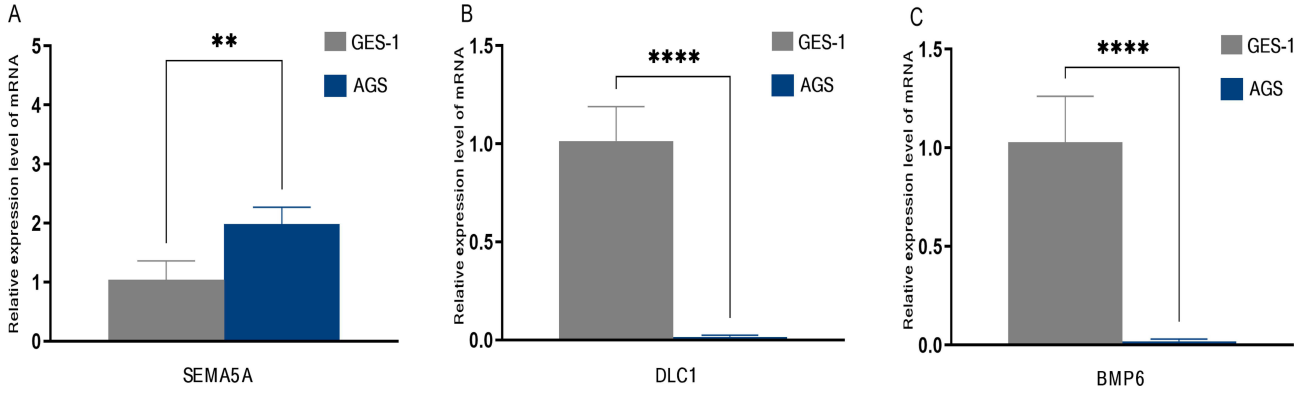

Figure 8 RT-qPCR results for the three genes (*SEMA5A*, *BMP6*, and *DLC1*) in AGS and GES-1. (**A**) The degree of *SEMA5A* mRNA expression. (**B**) *DLC1*'s mRNA expression level. (**C**) The degree of *BMP6* mRNA expression. * $p < 0.05$; ** $p < 0.01$; *** $p < 0.001$.**** $p < 0.0001$.

Discussion

The incidence of GC continues to rise annually, posing a significant threat to public health.[21] Although the 5-year survival rate for early-stage GC can exceed 95%, most cases are diagnosed at advanced stages, where the prognosis is poor and drug resistance is challenging.[22] For advanced GC, despite the widespread use of anti-angiogenic drugs, immunotherapies, and biologics, the median survival rarely exceeds 12 months.[23] Understanding the molecular mechanisms driving GC development is therefore essential for identifying therapeutic targets and devising effective treatments. Previous research has demonstrated that *SEMA5A* promotes GC invasion and metastasis through the ERK/MMP9 and PI3K/Akt/uPA signaling pathways.[6,7] Given that PI3K/Akt is a critical pathway in autophagy,[24] it is hypothesized that *SEMA5A* may regulate ARGs and thereby drive GC progression. The association between *SEMA5A* and ARGs is not well-explored in GC; however, *SEMA5A* has been identified as a hub gene potentially involved in the damage process of type 2 alveolar epithelial cells during acute respiratory distress syndrome by modulating autophagy.[25] This suggests that *SEMA5A* may influence autophagy-related molecular pathways in certain pathological contexts.

In this study, *SEMA5A* and its associated ARGs were identified through bioinformatics analysis, with their prognostic significance in GC assessed. Additionally, molecular regulatory mechanisms and immune infiltration patterns that may

contribute to GC progression were explored, offering valuable insights for further investigation into GC molecular mechanisms.

SEMA5A was significantly upregulated in GC samples compared to adjacent normal tissues. Survival and clinicopathological analyses demonstrated that high *SEMA5A* expression correlated with significantly worse outcomes, particularly at more advanced stages of GC. These results indicate that *SEMA5A* may play a critical role in GC development and is associated with poor prognosis, consistent with previous research. Notably, there is no existing report on whether *SEMA5A* regulates autophagy to promote GC development, prompting further analysis in conjunction with ARGs.

By intersecting DEGs with the ARGs set in the GC and control groups within the training set, 90 differentially expressed ARGs were identified. GO and KEGG analyses revealed significant enrichment of these ARGs in pathways related to the regulation of autophagy, positive regulation of autophagy, and macroautophagy, indicating their potential roles in either promoting or inhibiting GC progression through autophagy modulation. Correlation analysis further identified four ARGs (*TNFSF11, BMP6, ITPR1 and DLC1)* as characteristic genes, each exhibiting a correlation coefficient greater than 0.3 with *SEMA5A*. Prognostic evaluation of these genes highlighted *BMP6* and *DLC1* as key ARGs for subsequent analysis.

Further investigation revealed significantly lower expression levels of *DLC1* and *BMP6* in the GC group compared to the normal group, with marked upregulation in more advanced T stages, suggesting potential oncogenic properties for both genes. However, literature suggests that *DLC1*, as a GTPase-activating protein for Rho family members, plays a central role in cancer development and progression.[26,27] While *DLC1* is recognized as a potential tumor suppressor across various cancers,[28] its reduced expression in GC has been reported, albeit in studies with small sample Sizes.[29,30] The exact role and underlying mechanisms of *DLC1* in GC remain unclear. Moreover, some studies indicate that *DLC1* may inhibit the progression of liver, lung, and colorectal cancers by promoting autophagy,[29,31–33] though its impact on GC via autophagy regulation has not yet been reported.

BMP6, a member of the transforming growth factor-β (TGF-β) ligand superfamily, is implicated in regulating iron homeostasis, inhibiting invasion by enhancing adhesion and cell-cell interactions, and directly promoting angiogenesis in vascular endothelial cell.[34] *BMP6* is primarily considered a tumor suppressor, with its low expression closely associated with tumor progression. During tumorigenesis, *BMP6* binds to BMPR, activating intracellular Smad effectors, while gene silencing is predominantly mediated by methylation.[35] Additionally, Maria Catalina Gomez-Puerto et al demonstrated that BMPR2 can be degraded in primary human pulmonary artery endothelial cells (PAECs) via a lysosomal pathway related to autophagy.[36] Despite these findings, the role of *BMP6* in GC remains unexplored, and our study is the first to confirm its downregulation in GC via qPCR. In conclusion, the mechanisms by which *DLC1* and *BMP6* function in GC, particularly their potential roles in autophagy regulation and interaction with *SEMA5A*, remain inadequately understood and require further clinical and experimental investigation.

To explore the potential biological functions of *SEMA5A* and its associated ARGs, GSEA analyses were performed. The analysis revealed the co-enrichment of three genes within the ribosome pathway and ECM receptor interaction pathways. The ribosome pathway is implicated in the progression of various diseases, including malignant tumors, neurodegenerative disorders, hematological diseases, and congenital abnormalities.[37] Ribosomes play a pivotal role in cell autophagy, with ribosome autophagy (ribophagy) serving as a key mechanism for selective autophagy in eukaryotes. Wyant et al demonstrated that NUFIP1, in the context of starvation-induced ribophagy, is closely associated with ribophagy initiation and acts as a key receptor mediating this process.[38] The ECM receptor interaction pathway is integral to tumor cell proliferation and metastasis, as upregulation of ECM expression, commonly observed in tumor tissues, facilitates epithelial-mesenchymal transition, thereby enhancing tumor invasion and metastasis.[39,40] This pathway is also critically involved in tumorigenesis, cell detachment, adhesion, and metastasis.[41] These results suggest that *SEMA5A* and the two key genes form an interconnected network of pathways.

It is noteworthy that the potential influence of these three genes on the biological behavior of GC through the ribosome pathway and ECM receptor interaction pathway has not yet been reported, warranting further investigation.

Currently, immunotherapy has shown promising results in the clinical treatment of patients with GC, improving their prognosis.[42] However, a significant portion of patients with GC do not respond to immunotherapy.[43] Structural and functional alterations in genes play a critical role in immune escape and suppression within the tumor microenvironment

(TME), potentially regulating tumor development and progression directly.[44,45] Additionally, autophagy exerts a dual role, both inhibiting and promoting tumor formation as well as treatment resistance.[46] Studies have demonstrated that autophagy can modulate the immune response by influencing the release of immune cells and cytokines, with these effects primarily mediated by ARGs.[47] Further analysis of the differential expression of *SEMA5A* and key ARGs in the immune microenvironment of GC revealed a negative correlation between *SEMA5A, BMP6*, and M1 macrophages. Tumor-associated macrophages (TAMs) are emerging as pivotal players in GC development, with M1 and M2 TAMs, derived from circulating CCR2+ inflammatory monocytes, playing distinct roles. M1 TAMs primarily suppress GC progression by inhibiting pro-angiogenic and immune-promoting signaling pathways.[48] This suggests that *SEMA5A* and its associated ARGs, such as *DLC1* and *BMP6*, may inhibit M1 macrophage expression in the GC immune microenvironment, thereby promoting tumor progression. However, the specific mechanisms underlying this effect remain to be elucidated. Moreover, immune checkpoint analysis revealed significant differences in *HAVCR2* and *PDCD1LG2* expression between high and low *SEMA5A* expression groups, with higher levels observed in the former. *DLC1* showed the strongest correlation with *PDCD1LG2*. Current research indicates that the expression of immune checkpoint molecules can limit immune and anti-tumor responses, enabling tumor cells to evade immune surveillance.[49] Additionally, both immune and stromal cells were significantly upregulated in the *SEMA5A* high-expression group. These cell types, as major non-tumor components in the TME, are considered valuable for tumor diagnosis and prognostic assessment.[50] In summary, these results suggest that *SEMA5A, DLC1*, and *BMP6* may act as potential immunomodulatory genes involved in GC development and progression, potentially regulating GC through their impact on the immune microenvironment and immune response.

In this study, a ceRNA regulatory network was constructed, identifying key interaction pairs such as *NEAT1*-hsa-miR-5195-3p-*DLC1* and *SNHG16*-hsa-let-7d-5p-*SEMA5A*. These genes within the ceRNA network may play critical roles in influencing the prognosis of patients with GC, offering a rich pool of candidates for future research. Concurrently, a TF-mRNA regulatory network was established, including interactions like *ELK1-SEMA5A, RELA-DLC1*, and *FOXL1-BMP6*, with predicted TFs potentially binding to *SEMA5A, DLC1*, and *BMP6*. These findings provide critical evidence for further investigation into the biological processes of TF regulation of target genes and the pathogenesis of GC, aiding in the elucidation of GC's pre-transcriptional regulation models.

Finally, mRNA expression analysis confirmed that *SEMA5A* was significantly upregulated in AGS cells compared to GES-1 cells, while *DLC1* and *BMP6* exhibited the opposite trend. This consistency with our bioinformatics analysis suggests that *SEMA5A* is associated with poor GC prognosis, whereas *DLC1* and *BMP6* may be positively correlated with favorable prognosis. These results lay an important preliminary foundation for our subsequent studies.

Limitations

The RT-PCR technique was employed in this study to validate the expression of genes (*SEMA5A, DLC1, BMP6*). Although this method offers advantages such as high sensitivity and speed, it may exhibit variability in gene expression across different cells or tissues, potentially leading to inaccurate detection results. To address this, future research will involve establishing a tumor model in immunodeficient mice to investigate the specific functions of these genes and their interactions in an in vivo environment. This approach will allow for the observation of changes in tumor growth, metastasis, and survival, providing experimental data more reflective of physiological conditions and enhancing the biological relevance and credibility of the findings. Furthermore, considering that gene expression heterogeneity may be closely linked to disease status, prognosis, and treatment response, the next phase will involve collecting data from a broader range of clinical samples, including tumors at various stages and of different pathological types. This comprehensive analysis of *SEMA5A, DLC1*, and *BMP6* expression levels and their correlation with clinical characteristics aims to provide a more detailed understanding. By integrating in vivo functional studies with clinical sample validation, the biological functions and clinical significance of *SEMA5A, DLC1*, and *BMP6* can be explored in greater depth, thereby addressing the limitations of relying solely on RT-qPCR analysis and offering more comprehensive insights into their roles in disease mechanisms.

Conclusions

Ultimately, our investigation demonstrated that *SEMA5A* was increased in GC and was strongly associated with a poor outcome for GC, as validated by RT-qPCR validation and bioinformatics analysis. Furthermore, we discovered that *DLC1* and *BMP6* could be ARGs that are strongly associated with the expression of *SEMA5A* and have a significant prognostic value. Furthermore, by building a molecular network and analyzing immune infiltration, we were able to clarify the regulatory mechanism of *SEMA5A* and the related ARGs in GC. These results provide a vital theoretical framework for our later clinical investigation and experimental validation of the underlying biological process.

Data Sharing Statement

The relevant datasets for this study were obtained from the Gene Expression Omnibus (GEO) database (https://www.ncbi.nlm.nih.gov/geo/) and The Cancer Genome Atlas (TCGA) database (https://tcga-data.nci.nih.gov/tcga/). Duplicate genes were collected from the Gene Set Enrichment Analysis (GSEA) website (https://www.gsea-msigdb.org/gsea/index.jsp) and the Human Autophagy Database (HADb, http://www.autophagy.lu/index.html) after deletion of duplicate genes, ARGs were collected.

Ethics Approval and Informed Consent

The cell lines utilized in our research were procured from commercial sources. This study involving human data was reviewed and approved by the ethics committee of the First Affiliated Hospital of Kunming Medical University [(2024) Ethics L No. 136].

Author Contributions

All authors made a significant contribution to the work reported, whether that is in the conception, study design, execution, acquisition of data, analysis and interpretation; took part in drafting, revising or critically reviewing the article; gave final approval of the version to be published; have agreed on the journal to which the article has been submitted; and agree to be accountable for all aspects of the work.

Funding

This study was supported by National Natural Science Foundation of China, Joint Projects of Applied Basic Research of Kunming Medical University and Yunnan Province Science and Technology Department, Projects of Applied Basic Research of Yunnan Province Science and Technology Department (Serial number: 82260512; 202201AY070001-070; 202401AT070166).

Disclosure

The authors report no conflicts of interest in this work.

References

1. World Health Organization. Global cancer burden growing, amidst mounting need for services. *Saudi Med J*. 2024;45(3):326–327. PMID: 38438207.
2. Eusebi LH, Telese A, Marasco G, Bazzoli F, Zagari RM. Gastric cancer prevention strategies: A global perspective. *J Gastroenterol Hepatol*. 2020;35(9):1495–1502. doi:10.1111/jgh.15037
3. Purohit A, Sadanandam A, Myneni P, Singh RK. Semaphorin 5A mediated cellular navigation: Connecting nervous system and cancer. *Biochim Biophys Acta*. 2014;1846(2):485–493. doi:10.1016/j.bbcan.2014.09.006
4. Pan GQ, Ren HZ, Zhang SF, Wang XM, Wen JF. Expression of semaphorin 5A and its receptor plexin B3 contributes to invasion and metastasis of gastric carcinoma. *World J Gastroenterol*. 2009;15(22):2800–2804. doi:10.3748/wjg.15.2800
5. Pan G, Lv H, Ren H, et al. Elevated expression of semaphorin 5A in human gastric cancer and its implication in carcinogenesis. *Life Sci*. 2010;86(3–4):139–144. doi:10.1016/j.lfs.2009.12.004
6. Pan G, Zhang X, Ren J, et al. Semaphorin 5A, an axon guidance molecule, enhances the invasion and metastasis of human gastric cancer through activation of MMP9. *Pathol Oncol Res*. 2013;19(1):11–18. doi:10.1007/s12253-012-9550-8
7. Pan G, Zhu Z, Huang J, et al. Semaphorin 5A promotes gastric cancer invasion/metastasis via urokinase-type plasminogen activator/phosphoinositide 3-kinase/protein kinase B. *Dig Dis Sci*. 2013;58(8):2197–2204. doi:10.1007/s10620-013-2666-1
8. Debnath J, Gammoh N, Ryan KM. Autophagy and autophagy-related pathways in cancer. *Nat Rev Mol Cell Biol*. 2023;24(8):560–575. doi:10.1038/s41580-023-00585-z

9. Li X, He S, Ma B. Autophagy and autophagy-related proteins in cancer. *Mol Cancer*. 2020;19(1):12. doi:10.1186/s12943-020-1138-4
10. Yamamoto H, Matsui T. Molecular mechanisms of macroautophagy, microautophagy, and chaperone-mediated autophagy. *J Nippon Med Sch*. 2024;91(1):2–9. doi:10.1272/jnms.JNMS.2024_91-102
11. Cao Y, Luo Y, Zou J, et al. Autophagy and its role in gastric cancer. *Clin Chim Acta*. 2019;489:10–20. doi:10.1016/j.cca.2018.11.028
12. Lu SY, Guo S, Chai SB, et al. Autophagy in gastric mucosa: The dual role and potential therapeutic target. *Biomed Res Int*. 2021;2021:2648065. doi:10.1155/2021/2648065
13. Nabavi-Rad A, Yadegar A, Sadeghi A, et al. The interaction between autophagy, helicobacter pylori, and gut microbiota in gastric carcinogenesis. *Trends Microbiol*. 2023;31(10):1024–1043. doi:10.1016/j.tim.2023.04.001
14. Gao S, Tan H, Li D. Oridonin suppresses gastric cancer SGC-7901 cell proliferation by targeting the TNF-alpha/androgen receptor/TGF-beta signalling pathway axis. *J Cell Mol Med*. 2023;27(18):2661–2674. doi:10.1111/jcmm.17841
15. Gao S, Tan H, Gang J. Inhibition of hepatocellular carcinoma cell proliferation through regulation of the cell cycle, AGE-RAGE, and leptin signaling pathways by a compound formulation comprised of andrographolide, wogonin, and oroxylin A derived from andrographis paniculata (Burm.f.) Nees. *J Ethnopharmacol*. 2024;329:118001. doi:10.1016/j.jep.2024.118001
16. Gao S, Gang J, Yu M, Xin G, Tan H. Computational analysis for identification of early diagnostic biomarkers and prognostic biomarkers of liver cancer based on GEO and TCGA databases and studies on pathways and biological functions affecting the survival time of liver cancer. *BMC Cancer*. 2021;21(1):791. doi:10.1186/s12885-021-08520-1
17. Yang Y, Wang Y, Wang C, Xu X, Liu C, Huang X. Identification of hub genes of Parkinson's disease through bioinformatics analysis. *Front Neurosci*. 2022;16:974838. doi:10.3389/fnins.2022.974838
18. Zhang D, Zheng C, Zhu T, Yang F, Zhou Y. Identification of key module and hub genes in pulpitis using weighted gene co-expression network analysis. *BMC Oral Health*. 2023;23(1):2. doi:10.1186/s12903-022-02638-9
19. Hu X, Ni S, Zhao K, Qian J, Duan Y. Bioinformatics-led discovery of osteoarthritis biomarkers and inflammatory infiltrates. *Front Immunol*. 2022;13:871008. doi:10.3389/fimmu.2022.871008
20. Li WH, Han JR, Ren PP, Xie Y, Jiang DY. Exploration of the mechanism of Zisheng Shenqi decoction against gout arthritis using network pharmacology. *Comput Biol Chem*. 2021;90:107358. doi:10.1016/j.compbiolchem.2020.107358
21. Sung H, Ferlay J, Siegel RL, et al. Global cancer statistics 2020: GLOBOCAN estimates of incidence and mortality worldwide for 36 cancers in 185 countries. *CA Cancer J Clin*. 2021;71(3):209–249. doi:10.3322/caac.21660
22. Song Z, Wu Y, Yang J, Yang D, Fang X. Progress in the treatment of advanced gastric cancer. *Tumour Biol*. 2017;39(7):1010428317714626. doi:10.1177/1010428317714626
23. Petryszyn P, Chapelle N, Matysiak-Budnik T. Gastric cancer: Where are we heading? *Dig Dis*. 2020;38(4):280–285. doi:10.1159/000506509
24. Kma L, Baruah TJ. The interplay of ROS and the PI3K/Akt pathway in autophagy regulation. *Biotechnol Appl Biochem*. 2022;69(1):248–264. doi:10.1002/bab.2104
25. Chen H, Ding J, Xue H, Tang X, Yan Y, Xie Y. SnRNA-Seq analysis reveals ten hub genes associated with alveolar epithelial cell injury during pulmonary acute respiratory distress syndrome. *Heliyon*. 2023;9(6):e17160. doi:10.1016/j.heliyon.2023.e17160
26. Barras D, Widmann C. GAP-independent functions of DLC1 in metastasis. *Cancer Metastasis Rev*. 2014;33(1):87–100. doi:10.1007/s10555-013-9458-0
27. Ren G, Li G. Tumor suppressor gene DLC1: Its modifications, interactive molecules, and potential prospects for clinical cancer application. *Int J Biol Macromol*. 2021;182:264–275. doi:10.1016/j.ijbiomac.2021.04.022
28. Hinsenkamp I, Kohler JP, Flachsenhaar C, et al. Functional antagonism between CagA and DLC1 in gastric cancer. *Cell Death Discov*. 2022;8(1):358. doi:10.1038/s41420-022-01134-x
29. Wu HT, Xie CR, Lv J, et al. The tumor suppressor DLC1 inhibits cancer progression and oncogenic autophagy in hepatocellular carcinoma. *Lab Invest*. 2018;98(8):1014–1024. doi:10.1038/s41374-018-0062-3
30. Li F, Shang Y, Zhang H, She J, Wang G, Sun Q. Development of a novel autophagy-related gene prognostic signature for gastric cancer. *Transl Cancer Res*. 2021;10(6):2790–2800. doi:10.21037/tcr-21-191
31. Zhang Y, Li G. A tumor suppressor DLC1: The functions and signal pathways. *J Cell Physiol*. 2020;235(6):4999–5007. doi:10.1002/jcp.29402
32. Wang L, Jiang X, Zhang X, Shu P. Prognostic implications of an autophagy-based signature in colorectal cancer. *Medicine*. 2021;100(13):e25148. doi:10.1097/MD.0000000000025148
33. Liu Z, Zhang K, Zhao Z, Qin Z, Tang H. Prognosis-related autophagy genes in female lung adenocarcinoma. *Medicine*. 2022;101(1):e28500. doi:10.1097/MD.0000000000028500
34. Garcia Muro AM, Garcia Ruvalcaba A, de la Torre LDC R, Sanchez Lopez JY. Role of the BMP6 protein in breast cancer and other types of cancer. *Growth Factors*. 2021;39(1–6):1–13. doi:10.1080/08977194.2021.1994964
35. Liu G, Liu YJ, Lian WJ, Zhao ZW, Yi T, Zhou HY. Reduced BMP6 expression by DNA methylation contributes to EMT and drug resistance in breast cancer cells. *Oncol Rep*. 2014;32(2):581–588. doi:10.3892/or.2014.3224
36. Gomez-Puerto MC, van Zuijen I, Huang CJ, et al. Autophagy contributes to BMP type 2 receptor degradation and development of pulmonary arterial hypertension. *J Pathol*. 2019;249(3):356–367. doi:10.1002/path.5322
37. Ertekin E, Gencturk E, Kasim M, Ulgen KO. A drug repurposing and protein-protein interaction network study of ribosomopathies using yeast as a model system. *OMICS*. 2020;24(2):96–109. doi:10.1089/omi.2019.0096
38. Wyant GA, Abu-Remaileh M, Frenkel EM, et al. NUFIP1 is a ribosome receptor for starvation-induced ribophagy. *Science*. 2018;360(6390):751–758. doi:10.1126/science.aar2663
39. Andersen MK, Rise K, Giskeodegard GF, et al. Integrative metabolic and transcriptomic profiling of prostate cancer tissue containing reactive stroma. *Sci Rep*. 2018;8(1):14269. doi:10.1038/s41598-018-32549-1
40. Zhang QJ, Li DZ, Lin BY, Geng L, Yang Z, Zheng SS. SNHG16 promotes hepatocellular carcinoma development via activating ECM receptor interaction pathway. *Hepatobiliary Pancreat Dis Int*. 2022;21(1):41–49. doi:10.1016/j.hbpd.2021.09.006
41. Yan P, He Y, Xie K, Kong S, Zhao W. In silico analyses for potential key genes associated with gastric cancer. *PeerJ*. 2018;6:e6092. doi:10.7717/peerj.6092
42. Smyth EC, Nilsson M, Grabsch HI, van Grieken NC, Lordick F. Gastric cancer. *Lancet*. 2020;396(10251):635–648. doi:10.1016/S0140-6736(20)31288-5

43. Olino K, Park T, Ahuja N. Exposing hidden targets: Combining epigenetic and immunotherapy to overcome cancer resistance. *Semin Cancer Biol*. 2020;65:114–122. doi:10.1016/j.semcancer.2020.01.001
44. Joshi SS, Badgwell BD. Current treatment and recent progress in gastric cancer. *CA Cancer J Clin*. 2021;71(3):264–279. doi:10.3322/caac.21657
45. Tian R, Sun Y, Han X, et al. Identification and validation of prognostic autophagy-related genes associated with immune microenvironment in human gastric cancer. *Aging*. 2022;14(18):7617–7634. doi:10.18632/aging.204313
46. Silva VR, Neves SP, Santos LS, Dias RB, Bezerra DP. Challenges and therapeutic opportunities of autophagy in cancer therapy. *Cancers*. 2020;12 (11):3461. doi:10.3390/cancers12113461
47. Levine B, Kroemer G. Biological functions of autophagy genes: A disease perspective. *Cell*. 2019;176(1–2):11–42. doi:10.1016/j.cell.2018.09.048
48. Gambardella V, Castillo J, Tarazona N, et al. The role of tumor-associated macrophages in gastric cancer development and their potential as a therapeutic target. *Cancer Treat Rev*. 2020;86:102015. doi:10.1016/j.ctrv.2020.102015
49. Niu X, Ren L, Wang S, et al. High Prolyl 4-Hydroxylase subunit alpha 3 expression as an independent prognostic biomarker and correlated with immune infiltration in gastric cancer. *Front Genet*. 2022;13:952335. doi:10.3389/fgene.2022.952335
50. Wang R, Song S, Qin J, et al. Evolution of immune and stromal cell states and ecotypes during gastric adenocarcinoma progression. *Cancer Cell*. 2023;41(8):1407–1426e9. doi:10.1016/j.ccell.2023.06.005